Original Research Article

Extracts from *Tenebrio molitor* Larvae and *Protaetia brevitarsis* Larvae Reduced Cadmium-induced Ferroptosis and Cytotoxicity in Hep3B Cells

Pharmacognosy Magazine
1–11
© The Author(s) 2026
Article reuse guidelines:
in.sagepub.com/journals-permissions-india
DOI: 10.1177/09731296261444147
journals.sagepub.com/home/phm
Sage

Hyomin Lim[1], Yookyung Kim[2] and Woo-Jae Park[3]

Abstract

Background: Cadmium is a hepatotoxic heavy metal. Cadmium is known to induce ceramide generation and ferroptosis. Edible insects have recently been touted as a potential functional food. Various studies are being conducted in this regard.
Purpose: This study was designed to investigate whether two types of insects, *Tenebrio molitor* larvae (TM) and *Protaetia brevitarsis* larvae (PB), can inhibit cadmium-induced hepatotoxicity.
Materials and Methods: TM and PB powder were extracted using 70% ethanol and diluted with phosphate-buffered saline. TM and PB extracts were cotreated with cadmium in Hep3B cells. To investigate the mechanism, desipramine (an acid sphingomyelinase (ASMase) inhibitor), ferrostatin-1 (a ferroptosis inhibitor), and GW4869 (a neutral sphingomyelinase (NSMase) inhibitor) were used with cadmium. Anti-ferroptosis mechanisms of the TM and PB extracts were demonstrated using Western blot, enzyme-linked immunosorbent assay, MTT cell viability assay, real-time polymerase chain reaction analysis, and 2,2′-Azino-bis (3-ethylbenzothiazoline-6-sulfonic acid) diammonium salt (ABTS) radical scavenging assay.
Results: Cadmium increased ceramide generation and ferroptosis, concomitant with increased ASMase and NSMase expressions. To understand which mechanism is the upstream pathway, ferrostatin-1, desipramine, and GW4869 were treated with cadmium. Cadmium-induced hepatotoxicity was partially inhibited by ferrostatin-1, which did not affect ASMase expression and ceramide levels. Desipramine, but not GW4869, reduced cadmium-induced cell death and ferroptosis by reducing ceramide levels. Therefore, ceramide generation by ASMase can be an upstream pathway of ferroptosis in cadmium-induced cell death. Interestingly, TM and PB extracts reduced cadmium-induced ceramide increase and ASMase expression, leading to reduced ferroptosis and cell death. TM and PB extracts also had antioxidant properties due to their ability to scavenge reactive oxygen species.
Conclusion: TM and PB have an anti-ferroptosis mechanism against cadmium, which is due to inhibition of ceramide generation by reducing ASMase expression. Therefore, TM and PB can inhibit cadmium-induced hepatotoxicity as functional foods.

Keywords

Cadmium, ceramide, edible insects, ferroptosis, sphingomyelin phosphodiesterase

Received 18 February 2025; **revised** 03 December 2025; **accepted** 02 April 2026

Introduction

Cadmium is a toxic heavy metal that is released into the environment through various industrial activities, primarily from industrial and agricultural sources (Genchi et al., 2020). It is also found naturally in soil, minerals, and water and is particularly obtained as a byproduct of zinc production from ZnS (Charkiewicz et al., 2023). The half-life of cadmium in the human body is approximately 16–30 years (Charkiewicz et al., 2023). Cadmium induces various toxicities in the brain, heart, lungs, liver, kidney, bones, and reproductive system and has carcinogenic effects due to increased cell death (apoptosis,

[1]Department of Biochemistry, College of Medicine, Ewha Womans University, Gangseo-gu, Seoul, Republic of Korea
[2]Department of Human Ecology, Graduate School, Korea University, Seongbuk-gu, Seoul, Korea
[3]Department of Biochemistry, Chung-Ang University College of Medicine, Dongjak-gu, Seoul, Republic of Korea

Corresponding authors:
Woo-Jae Park, Department of Biochemistry, Chung-Ang University College of Medicine, 84 Heukseok-ro, Dongjak-gu, Seoul 06974, Republic of Korea.
E-mail: ooze@cau.ac.kr
Yookyung Kim, Department of Human Ecology, Graduate School, Korea University, 145 Anam-ro, Seongbuk-gu, Seoul 02841, Korea.
E-mail: yookyung_kim@korea.ac.kr

Creative Commons Non Commercial CC BY-NC: This article is distributed under the terms of the Creative Commons Attribution-NonCommercial 4.0 License (http://www.creativecommons.org/licenses/by-nc/4.0/) which permits non-Commercial use, reproduction and distribution of the work without further permission provided the original work is attributed as specified on the SAGE and Open Access pages (https://us.sagepub.com/en-us/nam/open-access-at-sage).

necrosis), epigenetic changes, DNA damage, oxidative stress, and abnormal DNA methylation (Charkiewicz et al., 2023). Cadmium induces reactive oxygen species (ROS) generation and mitochondrial dysfunction, leading to loss of mitochondrial membrane potential and caspase-3 activation (Gobe & Crane, 2010). Cadmium exposure exhibited hepatotoxicity and lipid accumulation in the liver (Xie et al., 2024). Inhibition of acid sphingomyelinase (ASMase) resulted in reduced cadmium-induced apoptosis and oxidative stress, thereby mitigating the associated liver damage (Xie et al., 2024).

Sphingolipids are essential lipids that play a crucial role in the structure of cell membranes, characterized by a sphingoid backbone (Park & Park, 2020). Palmitoyl-coenzyme A (CoA) and serine, via the *de novo* synthesis pathway, are combined with several enzymes in order to form ceramide (Park & Park, 2020). After synthesis, ceramide can be metabolized into a variety of substances, including sphingomyelin when phosphocholine is attached. Sphingomyelin is a component of cell membranes, and it can be hydrolyzed by Sphingomyelinases (SMase) to produce ceramide and phosphocholine (Truman et al., 2014). The activity of SMase is dependent on pH and cellular location, and it can be broadly divided into neutral sphingomyelinase (NSMase) and ASMase (Adada et al., 2016). The NSMase is highly expressed in the plasma membrane and plays a role in ceramide production in response to various signals. In contrast, the ASMase is predominantly located in lysosomes and regulates ceramide production by several stimuli, such as lipopolysaccharides (LPS), infections, alcohol, and Cu^{2+} (Adada et al., 2016).

Ferroptosis is an iron-dependent atypical form of cell death in which the cell membrane is disrupted by the accumulation of lipid peroxidation products (Xie et al., 2016). It is a mechanism that differs from necroptosis, pyroptosis, and apoptosis, in which cell death is triggered by accumulating iron and ROS (Xie et al., 2016). One of the main characteristics is the breakdown of the antioxidant system due to the degradation or deficiency of glutathione peroxidase 4 (GPX4), and the failure of GPX4 to reduce lipid peroxides leads to the accumulation of lipid peroxides, resulting in the breakdown of cell membranes and cell death (Xie et al., 2016). Erastin, a ferroptosis inducer, binds to voltage-dependent anion channel (VDAC)2 and VDAC3 and increases ROS generation (Xie et al., 2016). Furthermore, it also reduced glutathione (GSH) levels by inhibiting cysteine/glutamate antiporter system (Xie et al., 2016). Both effects increase ferroptosis.

In recent years, edible insects have emerged as a future food source. Edible insects are more environmentally friendly, producing less methane and carbon dioxide, and contain a variety of bioactive compounds with potential health benefits (Devi et al., 2022). In this study, we studied the effects of edible insects on the cadmium-induced hepatotoxicity.

Materials and methods

Materials

Tenebrio molitor (TM) and *Protaetia brevitarsis* (PB) larvae were obtained from Edible-bug (Busan, Korea) and GreenBugs Co-op. (Sokcho, Korea), respectively. The powder forms of TM and PB larvae were extracted using 70% ethanol at 4°C for 24 h. Extracts were diluted to a concentration of 200 mg/mL using 1× phosphate-buffered saline (PBS) and kept at −20°C for further use. Cadmium ($CdCl_2$), desipramine, GW4869, ferrostatin-1, 2,2′-Azino-bis (3-ethylbenzothiazoline-6-sulfonic acid) diammonium salt (ABTS), vitamin C, and anti-α-tubulin antibody (T9026) were purchased from Sigma–Aldrich (St. Louis, MO, USA). Erastin was obtained from Adooq Bioscience (Irvine, CA, USA). Anti-Slc7a11 antibody (12691) was obtained from Cell Signaling Technology (Beverly, MA, USA). Anti-Glutathione Peroxidase 4 (GPX4) antibody (ab125066) was purchased from Abcam (Cambridge, MA, USA). Anti-Mouse-Horseradish Peroxidase (HRP; 115-036-003) and anti-rabbit-HRP (111-035-003) antibodies were obtained from Jackson Laboratory (Bar Harbor, ME, USA).

Hep3B Cell Culture and Cadmium Treatment

Hep3B cells from an 8-year-old black male with liver cancer were cultured in Dulbecco's modified Eagle's medium (DMEM, Welgene, Korea) supplemented with 10% fetal bovine serum (Welgene) and 1% penicillin and streptomycin (Capricorn, Germany) at 37°C in a CO_2 incubator. Hep3B cells were subcultured every 2 days. For cadmium treatment, Hep3B cells were seeded to approximately 60%–70% confluency and treated with 1 or 10 μM of $CdCl_2$ for 24 h.

Western Blotting

Total proteins from Hep3B cells are extracted using radioimmunoprecipitation assay (RIPA) buffer (50 mM Tris–HCl, pH 7.5, 150 mM NaCl, 1% Nonidet P-40, 0.5% sodium deoxycholate, and 0.1% sodium dodecyl sulfate [SDS]) with the addition of protease and phosphatase inhibitors (Sigma–Aldrich) at a ratio of 200:1. In total, 50 μg of protein samples are loaded equally into each lane, separated using SDS-polyacrylamide gel electrophoresis (SDS-PAGE), and then transferred to Nitrocellulose (NC) membranes (Bio-Rad Laboratories, Hercules, CA, USA) through a wet transfer electrophoretic method. The membranes were incubated in a blocking buffer (5% bovine serum albumin in tris-based saline with 0.1% Tween-20 (TBST)) at 4°C. After blocking, the membranes were treated with primary antibody in TBST (1:1,000) overnight at 4°C, then with secondary antibodies (1:10,000) at room temperature for 1 h. Protein bands were visualized using the EzWestLumi Plus Reagent (ATTO Corp., Tokyo, Japan) and analyzed with the ChemiDoc MP Imaging System (Bio-Rad Laboratories).

MTT Cell Viability Assay

Hep3B cells were plated at a density of 3×10^4 cells per well in a 96-well plate, allowed to adhere for 18 h, and treated with 1 or 10 μM of $CdCl_2$ for 20 h. In some cases, Hep3B cells were treated with 1 μM ferrostatin-1, 2 μM desipramine, or 10 μM GW4869 for 24 h, followed by 1 μM of $CdCl_2$ for another 20 h. Finally, MTT solution was added to achieve a final concentration of 0.5 mg/mL to each well, and the cells were incubated for additional 4 h. After the media was removed, 200 μL of dimethyl sulfoxide was added to dissolve the purple formazan crystals. The resulting solution's absorbance was measured at 540 nm to determine cell viability.

Malondialdehyde (MDA), GSH, Ceramide, and ROS Measurement

The levels of MDA, GSH, and ceramide in Hep3B cells were measured using Lipid Peroxidation (MDA) Assay Kit (Abcam, Cambridge, MA, USA), GSH Assay Kit (Biovision, Milpitas, CA, USA), and Human Ceramide ELISA Kit (MyBioSource, San Diego, CA, USA), respectively. ROS was measured using DCFDA/H2DCFDA - Cellular ROS Assay Kit (Abcam).

Real-time Polymerase Chain Reaction (PCR)

Quantitative PCR was performed as previously described (Kim et al., 2023). The primers are summarized in Supplementary Table S1.

ABTS Radical Scavenging Assay

In total, 7.4 mM ABTS and 2.6 mM potassium sulfate were mixed in a ratio of 1:1. After 24 h, the mixture was diluted to an absorbance of 0.7 at 760 nm. Mixed 500 μL of the diluted solution with 100 μL of various concentrations of TM and PB extracts to obtain values. Vitamin C was used as a positive control due to its antioxidant property. The absorbance was measured using a spectrophotometer at 760 nm. The result was shown as median inhibitory concentration.

Total Phenolic Content and Flavonoid Content

Total phenolic content (TPC) was performed using the Folin–Ciocalteu method (Kim et al., 2025), and flavonoid content was performed as previously described (Cho et al., 2024). The results of TPC and flavonoid content were represented as mg of gallic acid equivalent per gram (mg GAE/g) and mg of quercetin equivalent per gram (mg QE/g), respectively.

Statistical Analyses

All experiments were repeated independently in triplicate, and values were expressed as mean ± standard error of the mean (SEM). Statistical significance was calculated using Tukey's *post hoc* test (GraphPad Prism 6.0; GraphPad Software, San Diego, CA). A statistical value of $p < .05$ was considered indicative of statistical significance.

Results

Cadmium Dose-dependently Increased Ferroptosis and Ceramide Generation

A previous study has reported that cadmium induces liver injury by increasing ceramide generation through ASMase (Xie et al., 2024). To explore this, we treated Hep3B cells with 1 or 10 μM of cadmium. The treatment dose-dependently increased the expression of ASMase, NSMase1, and NSMase2, with the most significant increase observed in ASMase (Figure 1A). Additionally, cadmium treatment led to an increase in ceramide levels (Figure 1B) and a decrease in cell viability (Figure 1C). Furthermore, cadmium treatment dose-dependently reduced the levels of GPX4 and soluble carrier family 7 member 11 (Slc7a11) proteins (Figure 1D), decreased GSH levels (Figure 1E), and increased MDA levels (Figure 1F), indicating that cadmium induces ceramide generation and ferroptosis.

Ferroptosis Inhibition Partially Reduced Cadmium-induced Toxicity

Since cadmium treatment induces ferroptosis (Figure 1), we administered ferrostatin-1, a ferroptosis inhibitor (Miotto et al., 2020). Ferrostatin-1 restored the levels of GPX4 and Slc7a11 (Figure 2A). It also partially reversed cadmium-induced cell death (Figure 2B) and recovered GSH levels (Figure 2C). Additionally, ferrostatin-1 reduced cadmium-induced MDA levels (Figure 2D). However, it had no effect on ASMase expression or ceramide levels (Figure 2E and 2F). These findings suggest that ferroptosis is not upstream of ceramide generation.

Cadmium Induces Ferroptosis via ASMase

To determine whether ceramide generation is upstream of ferroptosis, we utilized desipramine (an ASMase inhibitor) and GW4869 (an NSMase inhibitor). Desipramine not only recovered the protein levels of GPX4 and Slc7a11 (Figure 3A), but also enhanced cell viability and GSH levels (Figure 3B and 3C). It effectively inhibited ceramide generation (Figure 3D) and reduced both MDA levels and ROS generation (Figure 3E and 3F). These results indicate that ASMase inhibition mitigates cadmium-induced cell death and ferroptosis. On the other hand, GW4869, the NSMase inhibitor, failed to restore the levels of GPX4 and Slc7a11 (Figure 4A) and had no effect on cadmium-induced cell death (Figure 4B). Additionally, it did not recover the levels of GSH, ceramide,

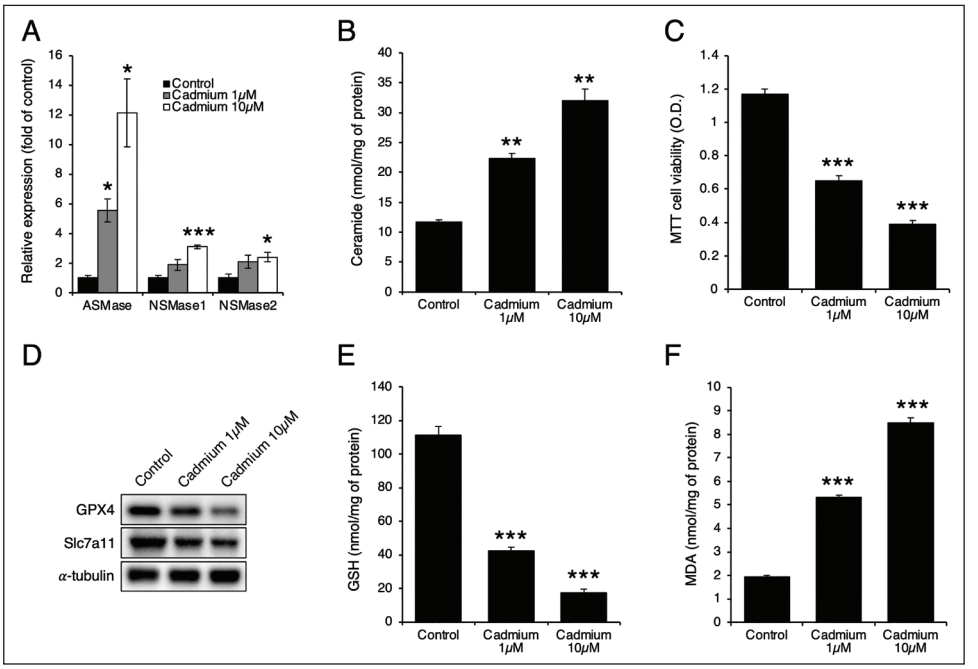


Figure 1. Effect of Cadmium on Ceramide Generation and Ferroptosis.

Notes: Hep3B cells were plated at 4 × 10^5 cells/well in a 6-well plate and treated with 1 or 10 μM of cadmium for 24 h. mRNA levels of ASMase, NSMase1, and NSMase2 (n = 3) (A), ceramide levels (n = 4) (B), MTT cell viability assay (n = 4) (C), representative Western blots of GPX4 and Slc7a11 (D), GSH levels (n = 4) (E), and MDA levels (n = 4) (F) were examined. Values are expressed as mean ± SEM compared to control group. All experiments were performed in triplicate. $^{*}p < .05$, $^{**}p < .01$, $^{***}p < .001$. ASMase: Acid sphingomyelinase, GSH: glutathione; MDA: Malondialdehyde; NSMase: Neutral sphingomyelinase.

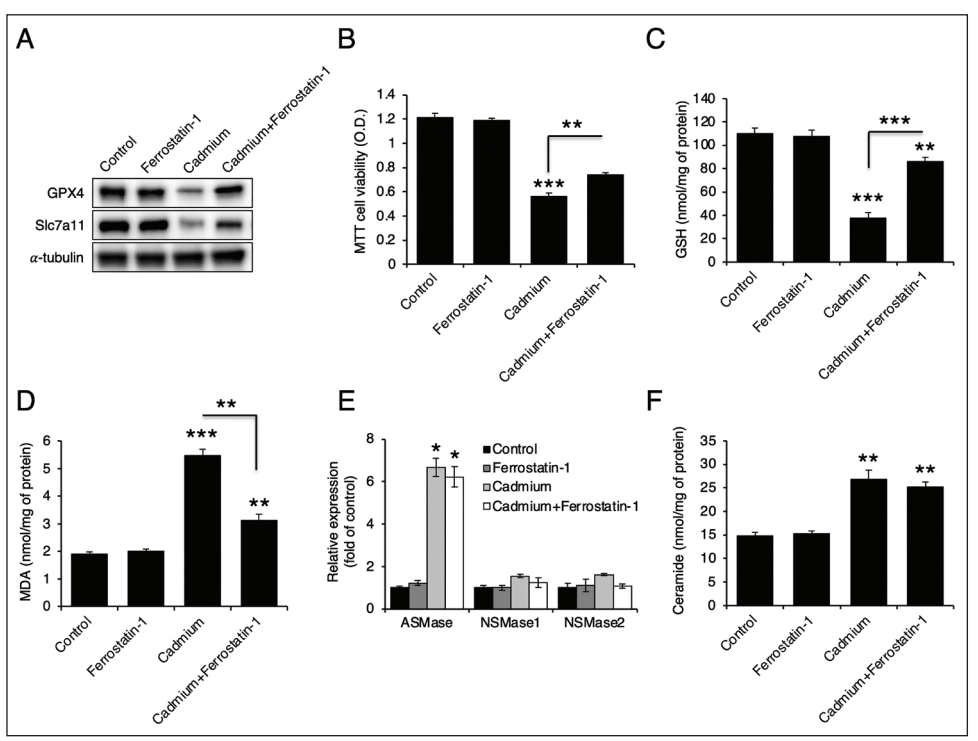


Figure 2. Inhibition of Ferroptosis Partially Recovers Cadmium-induced Toxicity.

Notes: Hep3B cells were plated at 4 × 10^5 cells/well in a 6-well plate and treated with 1 μM ferrostatin-1 for 24 h, followed by 1 μM of cadmium for another 24 h. Representative Western blots of GPX4 and Slc7a11 (A), MTT cell viability assay (n = 4) (B), GSH levels (n = 4) (C), MDA levels (n = 4) (D), mRNA levels of ASMase, NSMase1, and NSMase2 (n = 3) (E), and ceramide levels (n = 4) (F) were examined. Values are expressed as mean ± SEM compared to control group. All experiments were performed in triplicate. $^{**}p < .01$, $^{***}p < .001$. ASMase: Acid sphingomyelinase; GSH: Glutathione; MDA: Malondialdehyde; NSMase: Neutral sphingomyelinase.

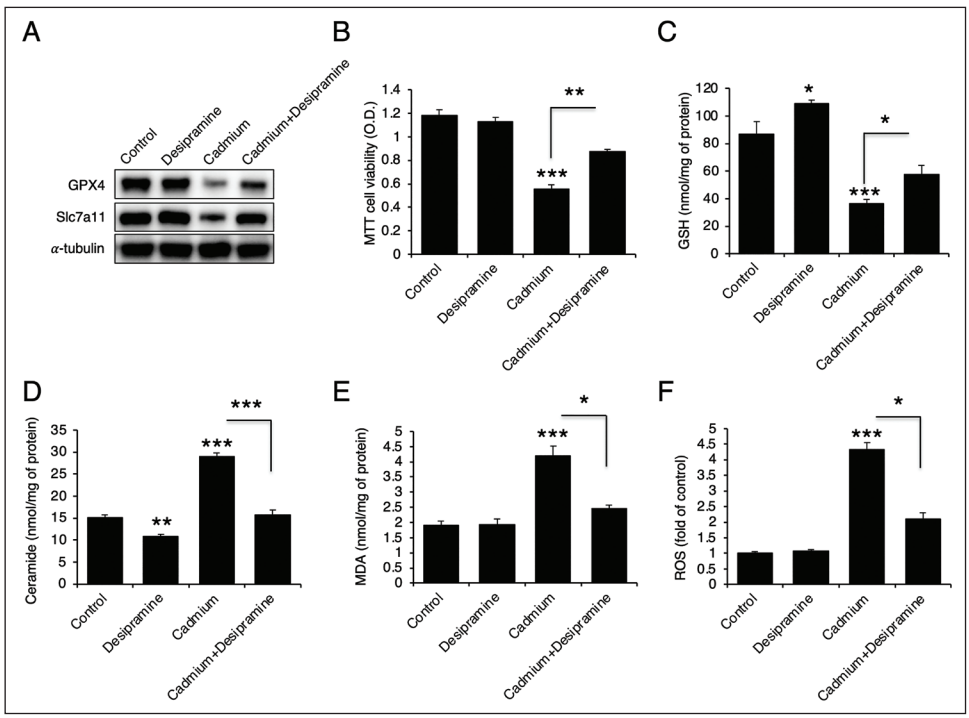


Figure 3. Inhibition of Acid Sphingomyelinase Partially Recovers Cadmium-induced Toxicity.

Notes: Hep3B cells were plated at 4 × 10^5 cells/well in a 6-well plate and treated with 2 μM desipramine for 24 h, followed by 1 μM of cadmium for another 24 h. Representative Western blots of GPX4 and Slc7a11 (A), MTT cell viability assay (B), GSH levels (C), ceramide levels (D), MDA levels (E), and ROS levels (F) were examined (n = 4). Values are expressed as mean ± SEM compared to control group. All experiments were performed in triplicate. $^{*}p < .05$, $^{**}p < .01$, $^{***}p < .001$. GSH: Glutathione; MDA: Malondialdehyde; ROS: Reactive oxygen species.

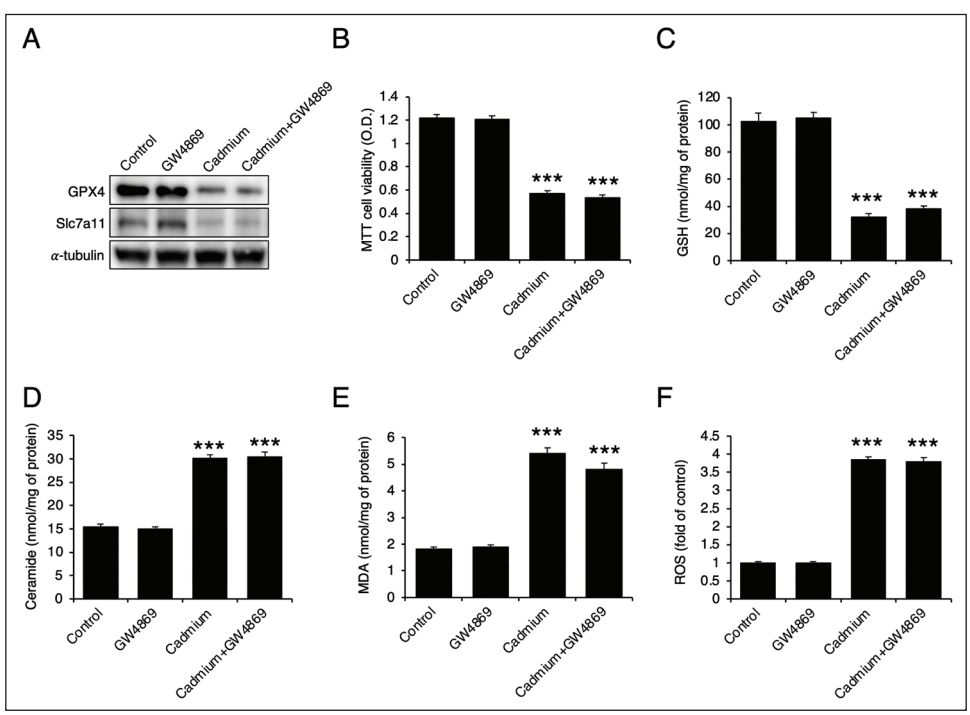


Figure 4. Inhibition of Neutral Sphingomyelinase Do Not Affect Cadmium-induced Toxicity.

Notes: Hep3B cells were plated at 4 × 10^5 cells/well in a 6-well plate and treated with 10 μM GW4869 for 24 h, followed by 1 μM of cadmium for another 24 h. Representative Western blots of GPX4 and Slc7a11 (A), MTT cell viability assay (B), GSH levels (C), ceramide levels (D), MDA levels (E), and ROS levels (n = 4) (F) were examined (n = 4). Values are expressed as mean ± SEM compared to control group. All experiments were performed in triplicate. $^{***}p < .001$. GSH: Glutathione; MDA: Malondialdehyde; ROS: Reactive oxygen species.

MDA, or ROS (Figure 4C–4F), suggesting that NSMase does not play a significant role in cadmium-induced cell death and ferroptosis.

TM Extract Prevents from Cadmium-induced Cell Death and Ferroptosis by Reducing the Expression of ASMase

Given that previous studies have demonstrated the inhibitory effects of extracts from certain edible insects (PB and *Gryllus bimaculatus* larvae) on ceramide generation (Park et al., 2022, 2024), we treated TM extract with cadmium. Initially, MTT assay was conducted over a range of concentrations to evaluate cytotoxicity induced by the extracts in the Hep3B cells. Both PB and TM extracts exhibited no detectable cytotoxicity at concentrations below 1,000 μg/mL (Supplementary Figure S1). Given that concentrations of 200 μg/mL were previously used in our anti-inflammatory and anti-sarcopenic studies (Oh et al., 2025; Park et al., 2024), we selected 200 μg/mL as the working concentration for the present experiments. Remarkably, TM extract downregulated ASMase expression (Figure 5A) and reduced ceramide generation (Figure 5B) in cadmium-treated Hep3B cells. It also inhibited cadmium-induced cell death (Figure 5C), partially restored GSH and MDA levels (Figure 5D and 5E), reduced ROS generation (Figure 5F), and improved the protein levels of GPX4 and Slc7a11 (Figure 5G). These findings suggest that TM extract mitigates cadmium-induced cell death and ferroptosis.

PB Extract Prevents from Cadmium-induced Cell Death and Ferroptosis by Reducing the Expression of ASMase

Because previous research demonstrated that PB extract inhibited LPS-induced ASMase expression (Park et al., 2024), we hypothesized that it might also suppress cadmium-induced ASMase expression. We treated PB extract with cadmium in Hep3B cells. Consistent with the results observed with TM, PB extracts inhibited cadmium-induced ASMase expression (Figure 6A) and ceramide generation (Figure 6B). Additionally, it reduced cadmium-induced cell death (Figure 6C) and restored GSH (Figure 6D) and MDA levels (Figure 6E). It also reduced ROS production (Figure 6F) and recovered the protein levels of GPX4 and Slc7a11 (Figure 6G).

TM Extract and PB Extracts Prevent from Erastin-induced Ferroptosis and Cell Death Due to Their Antioxidants Properties

Because both TM and PB extracts were effective in inhibiting cadmium-induced ferroptosis, we treated them in combination with erastin, a ferroptosis inducer (Thayyullathil et al., 2021), in Hep3B cells. Erastin significantly downregulated both GPX4 and Slc7a11 protein levels, but TM and PB extracts were able to recover these levels (Figure 7A). Erastin treatment also led to increased ASMase expression, ceramide generation, and MDA levels along with decreased cell viability and GSH levels (Figure 7B–7E). TM and PB extracts

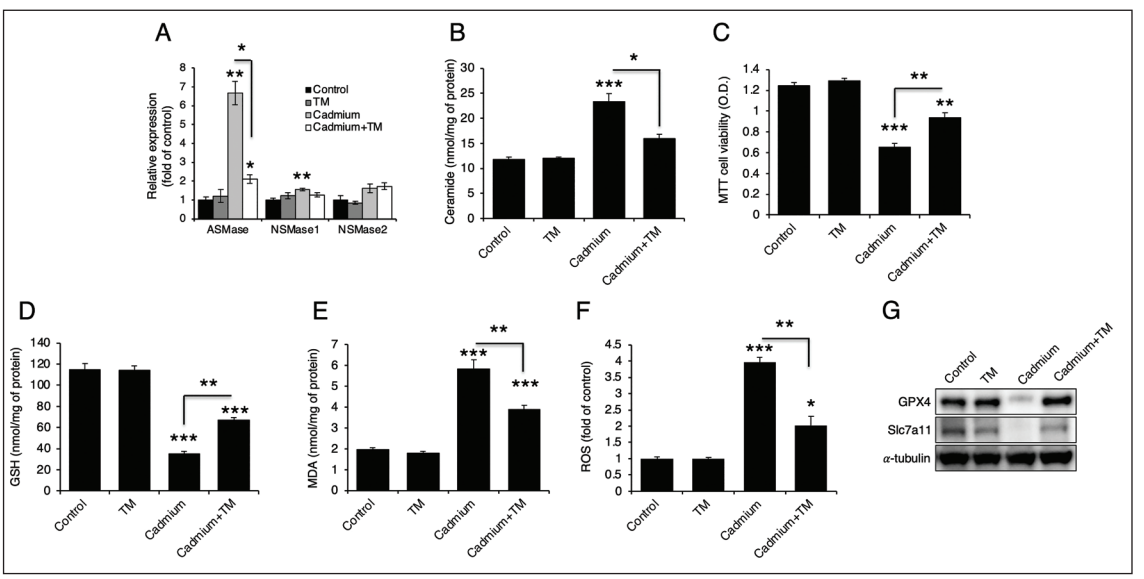


Figure 5. TM Extract Mitigates Cadmium-induced Toxicity by Reducing Ferroptosis.

Notes: Hep3B cells were plated at 4 × 10^5 cells/well in a 6-well plate and treated with 200 μg/mL TM extract for 24 h, followed by 1 μM of cadmium for another 24 h. mRNA levels of ASMase, NSMase1, and NSMase2 (n = 3) (A), ceramide levels (n = 4) (B), MTT cell viability assay (n = 4) (C), GSH levels (n = 4) (D), MDA levels (n = 4) (E), ROS levels (n = 4) (F), and representative Western blots of GPX4 and Slc7a11 (G) were examined. Values are expressed as mean ± SEM compared to control group. All experiments were performed in triplicate. $^{*}p < .05$, $^{**}p < .01$, $^{***}p < .001$. ASMase: Acid sphingomyelinase; GSH: Glutathione; MDA: Malondialdehyde; NSMase: Neutral sphingomyelinase; ROS: Reactive oxygen species; TM: *Tenebrio molitor* larvae.

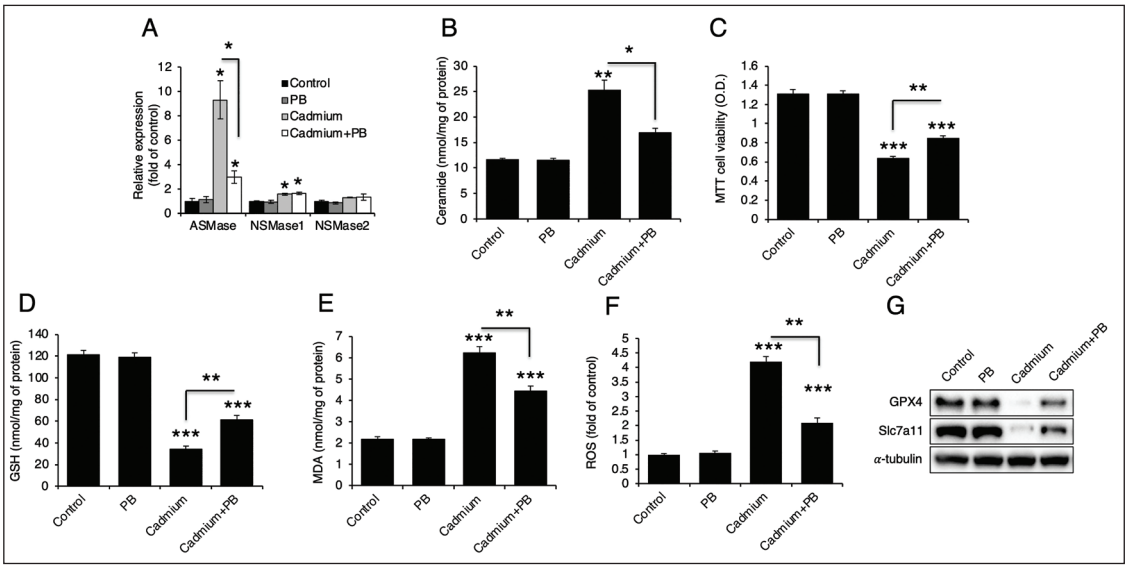


Figure 6. PB Extract Protects from Cadmium-induced Toxicity by Inhibiting Ferroptosis.

Notes: Hep3B cells were plated at 4 × 10^5 cells/well in a 6-well plate and treated with 200 μg/mL PB extract for 24 h, followed by 1 μM of cadmium for another 24 h. mRNA levels of ASMase, NSMase1, and NSMase2 (n = 3) (A), ceramide levels (n = 4) (B), MTT cell viability assay (n = 4) (C), GSH levels (n = 4) (D), MDA levels (n = 4) (E), ROS levels (n = 4) (F), and representative Western blots of GPX4 and Slc7a11 (G) were examined. Values are expressed as mean ± SEM compared to control group. All experiments were performed in triplicate. $^{*}p < .05$, $^{**}p < .01$, $^{***}p < .001$. ASMase: Acid sphingomyelinase; GSH: Glutathione; MDA: Malondialdehyde; NSMase: Neutral sphingomyelinase; PB: *Protaetia brevitarsis* larvae; ROS: Reactive oxygen species.

effectively reversed these effects, restoring ASMase expression, cell viability, and biochemical markers (Figure 7B–7E), suggesting that these extracts can mitigate erastin-induced ferroptosis and cell death.

Although TM and PB extracts inhibited cadmium-induced ferroptosis, they did not alter the protein levels of GPX4 and Slc7a11. This led us to hypothesize that these extracts possess antioxidant properties. To confirm this, we performed an ABTS radical scavenging assay. Both TM and PB extracts exhibited dose-dependent antioxidant effects (Figure 8). Furthermore, we quantified the levels of TPC and flavonoids in these extracts, and both TM and PB extracts were found to contain appreciable amounts of these bioactive components (Table 1).

Discussion

Cadmium is a hepatotoxic heavy metal, with chronic exposure leading to itai-itai disease (Inaba et al., 2005). Even at low doses, cadmium can cause liver damage by accumulating in the liver, ultimately resulting in liver fibrosis (Souza-Arroyo et al., 2022). In this study, we investigated the mechanism of acute cadmium toxicity in the liver. Previous studies have highlighted the impact of cadmium on sphingolipid metabolism (Lee et al., 2007; Xie et al., 2024; Xu et al., 2023). Cadmium induces ceramide production, which subsequently activates calpains and caspase-3 in the kidney proximal tubule cells (Lee et al., 2007) and increases ceramide and sphingomyelin contents in mouse midbrain (Xu et al., 2023). A recent study revealed that cadmium-induced ceramide generation is due to activated ASMase (Xie et al., 2024). Our findings also showed that cadmium activates ASMase, leading to increased ceramide production and ferroptosis. Furthermore, desipramine, an ASMase inhibitor, effectively inhibited cadmium-induced cell death and ferroptosis. On the other hand, ferrostatin-1, a ferroptosis inhibitor, partially inhibited cadmium-induced cell death and ferroptosis, but did not affect ASMase expression or ceramide levels. Additionally, erastin, a ferroptosis inducer, was found to activate ASMase, which plays an important role in GPX4 degradation (Du et al., 2023; Thayyullathil et al., 2021). Therefore, ceramide production driven by increased ASMase expression could be an upstream regulator of ferroptosis and play a significant role in cadmium-induced hepatotoxicity.

Cadmium causes hepatotoxicity through multiple mechanisms, including the generation of ROS, mitochondrial dysfunction, and ferroptosis (Rikans & Yamano, 2000). ROS can trigger ferroptosis by promoting lipid peroxidation, a process regulated by the GPX4 and Slc7a11 proteins (Xie et al., 2016). GPX4 is crucial in preventing lipid peroxidation by maintaining oxidized glutathione (GSSG) levels. The ferroptosis inducer erastin degrades GPX4, leading to reduced GSSG levels and increased lipid peroxidation (Xie et al., 2016). The cystine/glutamate antiporter, Slc7a11, also plays a critical role in this process by importing cystine, which is then reduced to cysteine and used for GSH synthesis (Lee & Roh, 2022). Depletion of Slc7a11 accelerates ferroptosis by reducing GSH levels. Extracts of TM and PB, known for their antioxidant properties (Ganguly et al., 2020; Lee et al., 2024;

Oh et al., 2022; Yoon et al., 2023), protect against cadmium- and erastin-induced ferroptosis, likely by reducing ROS levels. Although TM and PB extracts do not affect the basal expression of GPX4, SLC7A11, or ASMase, our findings demonstrate that they effectively restore these levels following cadmium exposure. This observation suggests that the extracts act primarily under conditions of oxidative or toxic stress rather than altering homeostatic sphingolipid or

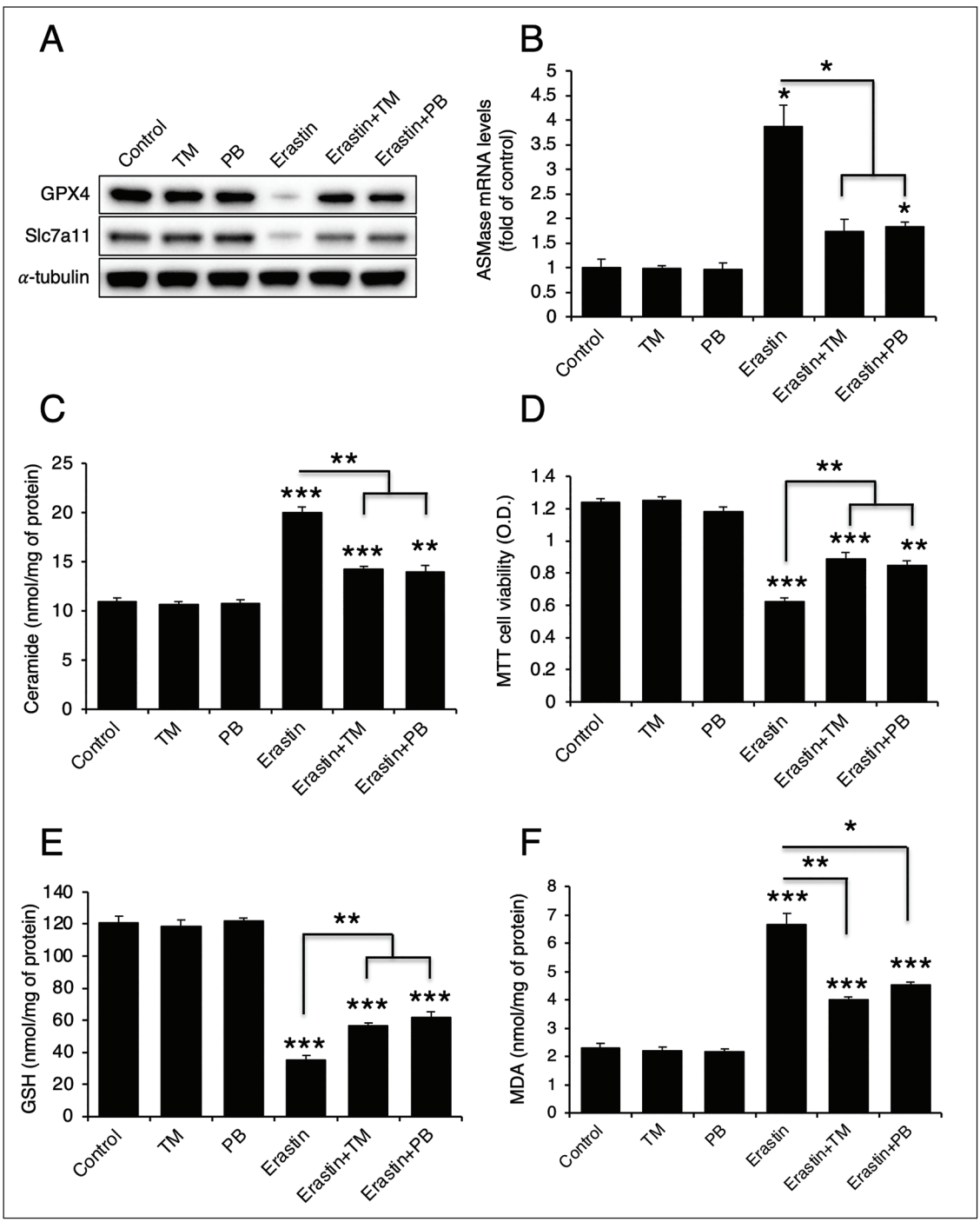


Figure 7. Both TM and PB Extracts Reduce Erastin-induced Ferroptosis.

Notes: Hep3B cells were plated at 4 × 10^5 cells/well in a 6-well plate and treated with 200 μg/mL TM or PB extracts for 24 h, followed by 20 μM of erastin for another 24 h. Representative Western blots of GPX4 and Slc7a11 (A), mRNA levels of ASMase (B), ceramide levels (C), MTT cell viability assay (D), GSH levels (E), and MDA levels (F) were examined (n = 4). Values are expressed as mean ± SEM compared to control group. All experiments were performed in triplicate. $^{*}p < .05$, $^{**}p < .01$, $^{***}p < .001$. ASMase: Acid sphingomyelinase; GSH: Glutathione; MDA: Malondialdehyde; PB: *Protaetia brevitarsis* larvae; TM: *Tenebrio molitor* larvae.

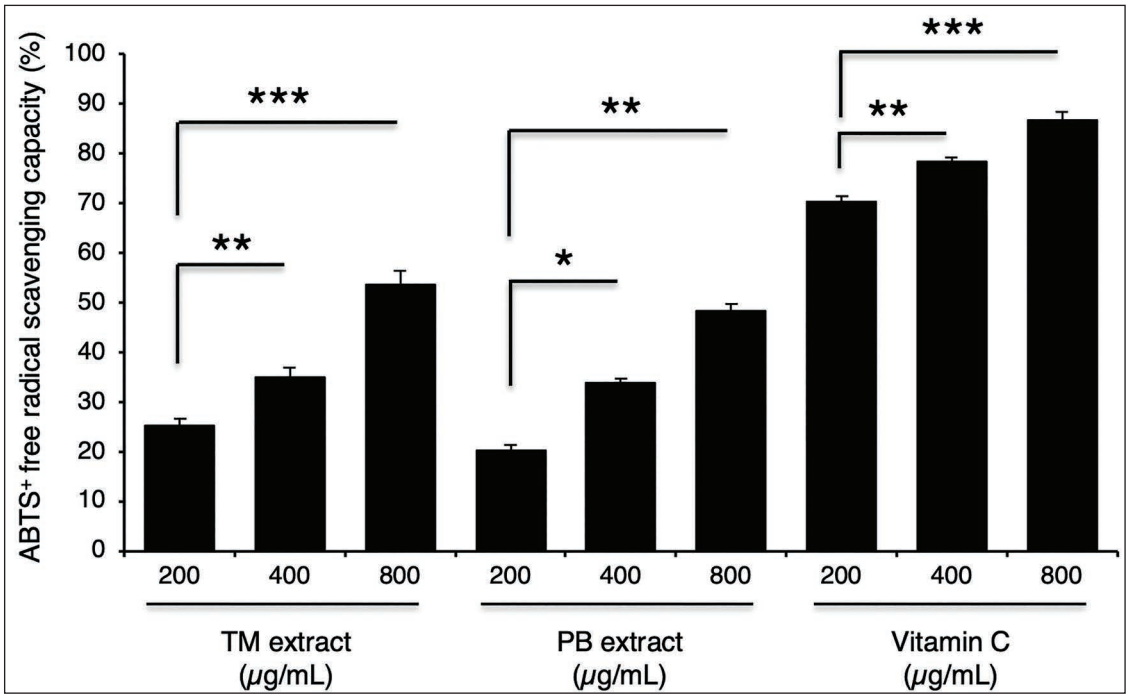


Figure 8. Both TM and PB Extracts Exhibit Antioxidant Properties. ABTS^{+} was Mixed with Various Concentrations of TM Extract, PB Extract, or Vitamin C (n = 4).

Notes: $^{*}p < .05$, $^{**}p < .01$, $^{***}p < .001$. PB: *Protaetia brevitarsis* larvae; TM: *Tenebrio molitor* larvae.

Table 1. Total Levels of Phenolic Content and Flavonoids in Extracts from *Tenebrio molitor* Larvae and *Protaetia brevitarsis* Larvae.

	Total Phenolic Content (mg GAE/g)	Flavonoid (mg QE/g)
Tenebrio molitor larvae	12.6 ± 0.45	3.65 ± 0.46
Protaetia brevitarsis larvae	13.64 ± 0.34	6.22 ± 0.71

ferroptosis-related pathways. The restoration of GPX4 and SLC7A11 is likely attributable, at least in part, to the antioxidant capacity of the extracts, which reduces intracellular ROS accumulation and thereby prevents the ROS-mediated degradation or suppression of these ferroptosis-regulating proteins. In addition, TM and PB extracts markedly attenuate the cadmium-induced upregulation of ASMase, a key enzyme that promotes ceramide generation and contributes to ferroptosis signaling. By suppressing this aberrant ASMase activation, the extracts may limit excessive ceramide accumulation and mitigate downstream cell-death pathways. Taken together, these findings indicate that both antioxidant activity and ASMase-modulatory effects cooperate to confer protection against cadmium-induced cytotoxicity and ferroptosis. This dual mode of action highlights the potential of TM and PB extracts as multifaceted modulators of oxidative stress and sphingolipid-mediated cell-death mechanisms. Other edible insects, such as *Gryllus bimaculatus* and *Allomyrina dichotoma* larvae, have also demonstrated antioxidant properties (Kim et al., 2020; Suh et al., 2010), suggesting that most edible insects may possess anti-ferroptosis effects. Because edible insects, including TM and PB, contain phenolic content and flavonoids (Nam et al., 2021; Nino et al., 2021; Yoon et al., 2020), they may contribute to antioxidant activity.

Both TM and PB, which are edible insects, have demonstrated beneficial effects on various diseases. TM is the most extensively studied, showing reductions in adipogenesis and obesity (Seo et al., 2017) and in the development of fatty liver (Ham et al., 2021). It also exhibits anti-inflammatory and antioxidant properties (Oh et al., 2022; Yoon et al., 2023). Fermented PB has been shown to protect against ethanol-induced hepatotoxicity (Lee et al., 2024), and protein hydrolysates from PB have demonstrated anti-obesity and hepatoprotective effects (Lee et al., 2022). Recently, we discovered that PB extract reduced LPS-induced ASMase expression in Hep3B cells (Park et al., 2024). Therefore, both TM and PB can be considered hepatoprotective agents that offer resistance against various toxic substances. Although TM and PB

extracts exhibit protective effects against cadmium-induced hepatotoxicity, their development as therapeutic agents beyond functional food applications remains challenging. This limitation arises from the compositional complexity of the extracts, which contain a diverse array of proteins, lipids, phenolic content, and flavonoids, making it difficult to determine which specific component mediates the observed protective effects. Therefore, future studies should prioritize the isolation and identification of the active bioactive compounds responsible for mitigating cadmium-induced hepatotoxicity.

Edible insects are emerging as a crucial future food resource, essential for reducing carbon emissions and promoting environmental sustainability (Devi et al., 2022). They are rich in various antioxidants, which have the effect of scavenging ROS and inhibiting ferroptosis. In particular, their ability to inhibit ceramide synthesis by downregulating ASMase expression is expected to have a protective effect against various liver diseases, such as fatty liver, Wilson's disease, and cadmium-induced liver fibrosis. Therefore, edible insects, such as TM and PB, hold much promise as a major hepatoprotective functional food in the future.

Abbreviations

ASMase: Acid sphingomyelinase; GPX4: Glutathione peroxidase 4; GSH: glutathione; LPS: Lipopolysaccharides; MDA: Malondialdehyde; NSMase: Neutral sphingomyelinase; PB: *Protaetia brevitarsis* larvae; ROS: Reactive oxygen species; Slc7a11: Soluble carrier family 7 member 11; SMase: Sphingomyelinase; TM: *Tenebrio molitor* larvae; TPC: Total phenolic content; VDAC: Voltage-dependent anion channel.

Data Availability Statement

The datasets generated during and/or analyzed during the current study are available from the corresponding author on reasonable request.

Declaration of Conflicting Interests

The authors declared no potential conflicts of interest with respect to the research, authorship, and/or publication of this article.

Ethical approval and informed consent

Not applicable.

Funding

The authors received no financial support for the research, authorship, and/or publication of this article.

Supplementary Material

Supplementary material for this article is available online.

ORCID iD

WooJae Park https://orcid.org/0000-0002-5770-7096

References

Adada, M., Luberto, C., & Canals, D. (2016). Inhibitors of the sphingomyelin cycle: Sphingomyelin synthases and sphingomyelinases. *Chemistry and Physics of Lipids*, *197*, 45–59. https://doi.org/10.1016/j.chemphyslip.2015.07.008

Charkiewicz, A. E., Omeljaniuk, W. J., Nowak, K., Garley, M., & Niklinski, J. (2023). Cadmium toxicity and health effects—A brief summary. *Molecules*, *28*(18), 6620. https://doi.org/10.3390/molecules28186620

Cho, E. C., Ahn, S., Hwang, H. J., Shin, K. O., Kim, S., & Choi, Y. J. (2024). Investigating the nutritional and functional properties of *Protaetia brevitarsis* larvae and isolated soy protein mixtures as alternative protein sources. *Foods*, *13*(10), 1540. https://doi.org/10.3390/foods13101540

Devi, W. D., Bonysana, R., Kapesa, K., Rai, A. K., Mukherjee, P. K., & Rajashekar, Y. (2022). Potential of edible insects as source of functional foods: Biotechnological approaches for improving functionality. *Systems Microbiology and Biomanufacturing*, *2*(3), 461–472. https://doi.org/10.1007/s43393-022-00089-5

Du, Y. X., Zhao, Y. T., Sun, Y. X., & Xu, A. H. (2023). Acid sphingomyelinase mediates ferroptosis induced by high glucose via autophagic degradation of GPX4 in type 2 diabetic osteoporosis. *Molecular Medicine*, *29*(1), 125. https://doi.org/10.1186/s10020-023-00724-4

Ganguly, K., Jeong, M.-S., Dutta, S. D., Patel, D. K., Cho, S.-J., & Lim, K.-T. (2020). *Protaetia brevitarsis* seulensis derived protein isolate with enhanced osteomodulatory and antioxidative property. *Molecules*, *25*(24), 6056. https://doi.org/10.3390/molecules25246056

Genchi, G., Sinicropi, M. S., Lauria, G., Carocci, A., & Catalano, A. (2020). The effects of cadmium toxicity. *International Journal of Environmental Research and Public Health*, *17*(11), 3782. https://doi.org/10.3390/ijerph17113782

Gobe, G., & Crane, D. (2010). Mitochondria, reactive oxygen species and cadmium toxicity in the kidney. *Toxicology Letters*, *198*(1), 49–55. https://doi.org/10.1016/j.toxlet.2010.04.013

Ham, J. R., Choi, R.-Y., Lee, Y., & Lee, M.-K. (2021). Effects of edible insect *Tenebrio molitor* larva fermentation extract as a substitute protein on hepatosteatogenesis and proteomic changes in obese mice induced by high-fat diet. *International Journal of Molecular Sciences*, *22*(7), 3615. https://doi.org/10.3390/ijms22073615

Inaba, T., Kobayashi, E., Suwazono, Y., Uetani, M., Oishi, M., Nakagawa, H., & Nogawa, K. (2005). Estimation of cumulative cadmium intake causing itai-itai disease. *Toxicology Letters*, *159*(2), 192–201. https://doi.org/10.1016/j.toxlet.2005.05.011

Kim, S.-H., Kim, Y., & Han, J.-S. (2020). Antioxidant activities and nutritional components of cricket (*Gryllus bimaculatus*) powder and protein extract. *Asian Journal of Beauty and Cosmetology*, *18*(2), 163–172. https://doi.org/10.20402/ajbc.2020.0016

Kim, S.-J., Park, W.-J., Choi, W., Kim, H. S., & Kim, Y. (2025). Supercritical CO2 defatting and hydrolysis improve the bioactivity of *Protaetia brevitarsis* seulensis proteins against oxidative stress, inflammation, and muscle atrophy. *Food Bioscience*, *74*, 107811. https://doi.org/10.1016/j.fbio.2025.107811

Kim, S.-J., Seo, I., Kim, M. H., Park, J.-W., Kim, S., & Park, W.-J. (2023). Ceramide synthase 4 overexpression exerts oncogenic properties in breast cancer. *Lipids in Health and Disease*, *22*(1), 183. https://doi.org/10.1186/s12944-023-01930-z

Lee, E. H., Chun, S. Y., Yoon, B., Han, M.-H., Chung, J.-W., Ha, Y.-S., Lee, J. N., Kim, H. T., Kim, D. H., Beik, G. Y., Ik Jang, B., Kwon, T. G., Park, C.-E., Lee, I.-S., Kim, B. S., & Lee, S.-O. (2022). Antiobesity and hepatoprotective effects of protein hydrolysates derived from *Protaetia brevitarsis* in an obese mouse model. *BioMed Research International*, *2022*, 4492132. https://doi.org/10.1155/2022/4492132

Lee, H. L., Kim, J. M., Go, M. J., Joo, S. G., Kim, T. Y., Lee, H. S., Hui Kim, J., Son, J.-S., & Heo, H. J. (2024). Fermented *Protaetia brevitarsis* larvae ameliorates chronic ethanol-induced hepatotoxicity in mice via AMPK and TLR-4/TGF-β1 pathways. *Journal of Microbiology and Biotechnology*, *34*(3), 606–621. https://doi.org/10.4014/jmb.2310.10003

Lee, J., & Roh, J.-L. (2022). SLC7A11 as a gateway of metabolic perturbation and ferroptosis vulnerability in cancer. *Antioxidants (Basel)*, *11*(12), 2444. https://doi.org/10.3390/antiox11122444

Lee, W.-K., Torchalski, B., & Thévenod, F. (2007). Cadmium-induced ceramide formation triggers calpain-dependent apoptosis in cultured kidney proximal tubule cells. *American Journal of Physiology-Cell Physiology*, *293*(3), C839–C847. https://doi.org/10.1152/ajpcell.00197.2007

Miotto, G., Rossetto, M., Di Paolo, M. L., Orian, L., Venerando, R., Roveri, A., Vučković, A.-M., Travain, V. B., Zaccarin, M., Zennaro, L., Maiorino, M., Toppo, S., Ursini, F., & Cozza, G. (2020). Insight into the mechanism of ferroptosis inhibition by ferrostatin-1. *Redox Biology*, *28*, 101328. https://doi.org/10.1016/j.redox.2019.101328

Nam, K. J., Eun-Jeong, J., & Yong-Suk, K. (2021). Antioxidant components and antioxidant activities of mealworm (*Tenebrio molitor* Larvae). *Journal of Food Hygiene and Safety*, *36*(1), 86–92.

Nino, M. C., Reddivari, L., Osorio, C., Kaplan, I., & Liceaga, A. M. (2021). Insects as a source of phenolic compounds and potential health benefits. *Journal of Insects as Food and Feed*, *7*(7), 1077–1088. https://doi.org/10.3920/JIFF2020.0113

Oh, E., Kim, M. H., Park, W.-J., & Kim, Y. (2025). Sustainable mealworm tofu as a dietary strategy to prevent muscle atrophy induced by dexamethasone in cellular and animal models. *Food Hydrocolloids for Health*, *7*, 100211. https://doi.org/10.1016/j.fhfh.2025.100211

Oh, E., Park, W.-J., & Kim, Y. (2022). Effects of *Tenebrio molitor* larvae and its protein derivatives on the antioxidant and anti-inflammatory capacities of tofu. *Food Bioscience*, *50*, 102105. https://doi.org/10.1016/j.fbio.2022.102105

Park, I. B., Kim, M. H., Han, J.-S., & Park, W.-J. (2022). *Gryllus bimaculatus* extract protects against palmitate-induced β-cell death by inhibiting ceramide synthesis. *Applied Biological Chemistry*, *65*(1), 72. https://doi.org/10.1186/s13765-022-00742-6

Park, W. J., Oh, E., & Kim, Y. (2024). *Protaetia brevitarsis* larvae extract protects against lipopolysaccharides-induced ferroptosis and inflammation by inhibiting acid sphingomyelinase. *Nutrition Research and Practice*, *18*(5), 602–616. https://doi.org/10.4162/nrp.2024.18.5.602

Park, W. J., & Park, J. W. (2020). The role of sphingolipids in endoplasmic reticulum stress. *FEBS Letters*, *594*(22), 3632–3651. https://doi.org/10.1002/1873-3468.13863

Rikans, L. E., & Yamano, T. (2000). Mechanisms of cadmium-mediated acute hepatotoxicity. *Journal of Biochemical and Moleculer Toxicology*, *14*(2), 110–117. https://doi.org/10.1002/(sici)1099-0461(2000)14:2<110::aid-jbt7>3.0.co;2-j

Seo, M., Goo, T. W., Chung, M. Y., Baek, M., Hwang, J. S., Kim, M. A., & Yun, E. Y. (2017). *Tenebrio molitor* larvae inhibit adipogenesis through AMPK and MAPKs signaling in 3T3-L1 adipocytes and obesity in high-fat diet-induced obese mice. *International Journal of Molecular Sciences*, *18*(3), 518. https://doi.org/10.3390/ijms18030518

Souza-Arroyo, V., Fabián, J. J., Bucio-Ortiz, L., Miranda-Labra, R. U., Gomez-Quiroz, L. E., & Gutiérrez-Ruiz, M. C. (2022). The mechanism of the cadmium-induced toxicity and cellular response in the liver. *Toxicology*, *480*, 153339. https://doi.org/10.1016/j.tox.2022.153339

Suh, H. J., Kim, S. R., Lee, K. S., Park, S., & Kang, S. C. (2010). Antioxidant activity of various solvent extracts from *Allomyrina dichotoma* (Arthropoda: Insecta) larvae. *Journal of Photochemistry and Photobiology B: Biology*, *99*(2), 67–73. https://doi.org/10.1016/j.jphotobiol.2010.02.005

Thayyullathil, F., Cheratta, A. R., Alakkal, A., Subburayan, K., Pallichankandy, S., Hannun, Y. A., & Galadari, S. (2021). Acid sphingomyelinase-dependent autophagic degradation of GPX4 is critical for the execution of ferroptosis. *Cell Death & Disease*, *12*(1), 26. https://doi.org/10.1038/s41419-020-03297-w

Truman, J.-P., Garcia-Barros, M., Obeid, L. M., & Hannun, Y. A. (2014). Evolving concepts in cancer therapy through targeting sphingolipid metabolism. *Biochimica et Biophysica Acta (BBA)—Molecular and Cell Biology of Lipids*, *1841*(8), 1174–1188. https://doi.org/10.1016/j.bbalip.2013.12.013

Xie, Y., Hou, W., Song, X., Yu, Y., Huang, J., Sun, X., & Tang, D. (2016). Ferroptosis: Process and function. *Cell Death & Differentiation*, *23*(3), 369–379. https://doi.org/10.1038/cdd.2015.158

Xie, D., Yan, J., Zhang, H., Zhang, H., Nie, G., Zhu, X., & Li, X. (2024). Cadmium exacerbates liver injury by remodeling ceramide metabolism: Multiomics and laboratory evidence. *Science of the Total Environment*, *923*, 171405. https://doi.org/10.1016/j.scitotenv.2024.171405

Xu, Y., Hong, H., Lin, X., Tong, T., Zhang, J., He, H., Yang, L., Mao, G., Hao, R., Deng, P., Yu, Z., Pi, H., Cheng, Y., & Zhou, Z. (2023). Chronic cadmium exposure induces Parkinson-like syndrome by eliciting sphingolipid disturbance and neuroinflammation in the midbrain of C57BL/6J mice. *Environmental Pollution*, *337*, 122606. https://doi.org/10.1016/j.envpol.2023.122606

Yoon, C. H., Jeon, S. H., Ha, Y. J., Kim, S. W., Bang, W. Y., Bang, K. H., Gal, S. W., Kim, I. S., & Cho, Y. S. (2020). Functional chemical components in *Protaetia brevitarsis* larvae: Impact of supplementary feeds. *Food Science of Animal Resources*, *40*(3), 461–473. https://doi.org/10.5851/kosfa.2020.e25

Yoon, Y., Oh, E., Park, W.-J., Kim, H. S., & Kim, Y. (2023). Effects of enzymatic hydrolysis and size fractionation of mealworm (*Tenebrio molitor* larvae) protein on antioxidant and anti-inflammatory activities and inhibition of muscle loss. *ACS Food Science & Technology*, *3*(5), 850–857. https://doi.org/10.1021/acsfoodscitech.3c00034